Back Electromotive Force Analysis of Outer-Rotor Hybrid Excitation Flux Switching Motor

Gadafi M. Romalan, Md Zarafi Ahmad, Siti Khalidah Rahimi and Kausalya Nadaraja
Research Center for Applied Electromagnetics (EMCenter), Universiti Tun Hussein Onn Malaysia, Batu Pahat, Malaysia
Department of Electrical Power Engineering, FKEE Universiti Tun Hussein Onn Malaysia Batu Pahat, Malaysia
dapiida@yahoo.com

***Abstract*—Outer-rotor machine installed for in-wheel drive electric vehicles becomes trending nowadays. Previously, outer-rotor hybrid excitation flux switching motor (OR-HEFSM) in wheel drive has been proposed to eliminate the transmission gear conventionally used in single drive electric vehicles. However, the back EMF of existing OR-HEFSM is not purely sinusoidal waveform due to harmonic content and high level of cogging torque. This kind of problem might be lead to create noise and tremor in the motor. In this paper, rotor pole skewing technique is adopted to improve back EMF waveform, harmonic content and cogging torque. The analyses carried out based on 2D FEA and 3D FEA using JMAG Designer Version 14.0. Besides, the flux linkage, flux distribution and output performances are also investigated. The results obtained show that the skewing method has improved the back-EMF waveform and reduce the cogging torque. The 3D FEA result indicates the peak to peak value of cogging torque has reduced by 91.42% with skewed rotor method. The torque and power performance of 3D-FEA has maximum values of 248.33Nm with 44.42% and 162.79kW with 33.42%, respectively in which higher when compared with 2D-FEA and skewing.**

***Index Terms*—Outer-Rotor; Hybrid Excitation Flux Switching Motor; Cogging Torque; Skewing.**

I. INTRODUCTION

Transportation is one of the critical issues in our daily life to be encounter and important to be managed properly in each stage of human civilization. It is classified into three groups such as land, sea and air transportation. Many inventors have planned and executed their creativity with various designs of vehicles for transportation. A demand for individual transit was raised greatly as growing number of people of the globe [1]. Unfortunately, increase number of transportation leads to serious problems with the environmental issues called global warming. The climate change of heat of the atmosphere is connected with a greenhouse gasses which is a form of water, vapor, carbon dioxide, methane, nitrous oxide, and ozone. Factors such as carbon dioxide, air pollutants, and greenhouse gasses are entering, then combine with the earth's atmosphere to contribute the global warming are present [2]. Apart from that, the primary causes of global warming increased by human being activities like sources of carbon dioxide emissions by using internal combustion engine (ICE) of vehicles for the transportation sector from fossil fuels combustion. So, the hybrid electric vehicle (HEVS) is a better solution to mitigate the carbon dioxide (CO_2) emission from transportation [3].

Presently, a tendency of using outer rotor in-wheel drive motors for electric vehicles (EVs) are suitable because of convenience in transmission gear system abolition resulting lighter vehicle, autonomous wheel manages, and plan developing traction batteries scope in the vast propulsive space. The brushless permanent magnet (PM) motor can generate low acoustic noise, low torque ripple, and high efficiency which accommodated the qualification for EVs momentum system [4]. In additional, Hybrid Excitation-Flux Switching Motor (HE-FSM) consisting active parts such as PMs, armature coil and field excitation coil (FEC) as a major flux source contrast to Permanent Magnet-Flux Switching Magnet (PM-FSM). The higher torque density, speed as well as power and efficiency are suitable in an outer-rotor arrangement for direct drive implementation compared to the inner-rotor configuration. Moreover, the preferences to direct torque control to the wheel, higher reliability and efficiency is one of the suitable candidates for in-wheel drive applications [5],[6].

II. HYBRID EXCITATION FLUX SWITCHING MOTOR

Flux Switching Motor (FSM) with a single structure of rotor has an iron core for easy manufacturing and robust. These give advantages that all brushes are ignored although; the entire domination is preserved over the field flux. The word of flux switching is established because of by changeable from the direction of a magnetic or electric field of the flux linkage by subsequent the moving of salient rotor pole. The whole excitation sources are on the stator with the field and armature assign to replacement stator teeth. The stator in the motor produces flux along a permanent magnet or by dc current flowing in the field winding. Furthermore, the FEC also is able to manage the changes of flux capability and also has the possibility to provide higher torque and power when accommodated on the stator part [5], [7], [8].

On the other hand, hybrid excitation motors (HEMs) consist of permanent magnets (PM) and field excitation coils (FEC) as their main flux source. HEMs are generally classified into four types. The first type is consisting of both PM and DC FEC fixed in rotor part whereas the armature coil is placed in stator bodies. The second type consists of PM in the rotor while DC FEC in the stator. Moreover, the third type composed of PM in the rotor and DC FEC in the motor end. Lastly, the fourth HEMs are the machine with both PM and DC FEC placed in the stator. Besides, the hybrid-excited flux-switching motor is explored and has potential to operate at high speeds because all the active parts are housed in the stator [9].

All HEMs stated in the first three consists of a PM in the rotor and can be categorized as "hybrid rotor-PM with FEC machines" while the final machine can be referred as "hybrid stator-PM with FEC machines". Based on its principles of operation, the fourth type is also known as "hybrid excitation flux switching motor" (HEFSM) which is getting more popular nowadays. HEFSM also utilized primary excitation by PMs as well as DC FEC as a secondary source. Based on various combinations of stator slots and rotor poles for HEFSMs have been tried. HEFSM requires significantly fewer magnets and has higher torque density to adjust the main flux. HEFSM also was developed to improve the starting or low-speed torque and high-speed flux-weakening capabilities, which are required in HEV [10].

III. Performances and Results Based on 2D and 3D Finite Element Analysis

In this study, the analysis is carried out using JMAG Designer version 14.0 with the design of OR-HEFSM has 12 stator slot 10 rotor pole. The 2-D FEA and 3-D FEA investigation are carried out to analyses the performances at no load analysis such as cogging torque, flux linkage, flux distribution, back-EMF, and harmonic of back-EMF. Then, on load analysis performances such as torque characteristic at numerous current densities, torque and power versus speed are also investigated. Figures 1, 2 and 3 show the design cross-sectional view of 2D, 3D and Skewing of OR-HEFSM.

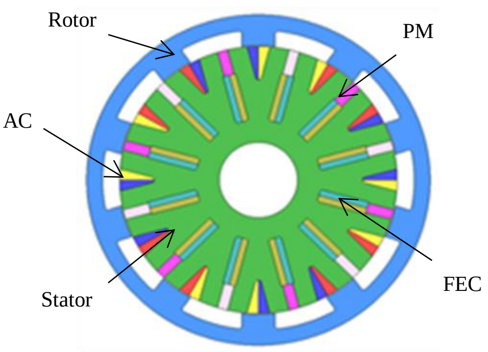

Figure 1: Cross-sectional view of 2D OR-HEFSM

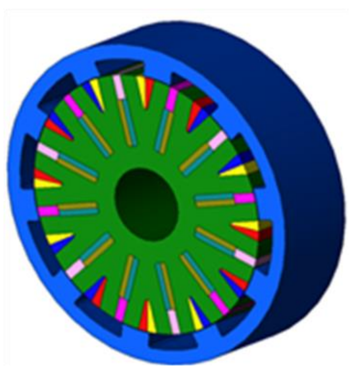

Figure 2: Cross-sectional view of 3D OR-HEFSM with original rotor structure

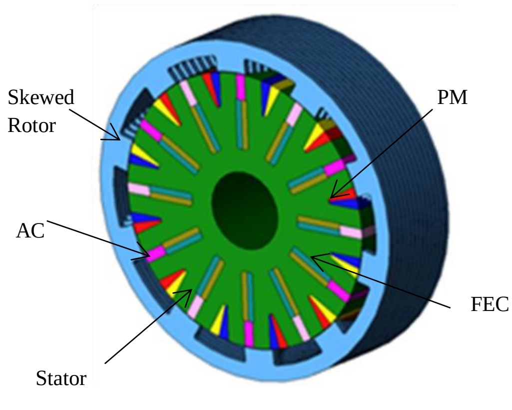

Figure 3: 3D cross-sectional view of OR-HEFSM with rotor skewing structure

A. Cogging Torque

The cogging or detent torque graph of 2D, 3D and the skew rotor is shown in Figure 4. The graph shows 6 cycles peak to peak of cogging torque of 2D, 3D, and skewed rotor at field current density, J_e of 30A/mm^2 is 80.52 Nm, 123.15 Nm and 10.57Nm, respectively. It is clear that the 3D analysis has the highest peak-to-peak cogging torque due to the highest volume consideration. The higher the cogging torque will create higher noise and cause the motor to vibrate. On the other hand, by applying the skewing technique on the rotor, the peak-to-peak cogging torque of the motor has reduced greatly with 91% reduction.

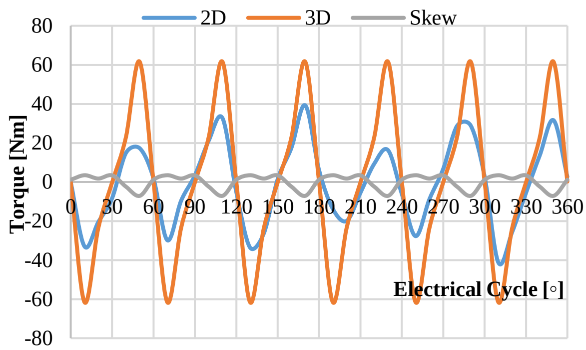

Figure 4: Cogging torque of 2D, 3D and skew rotor at Je of 30A/mm2

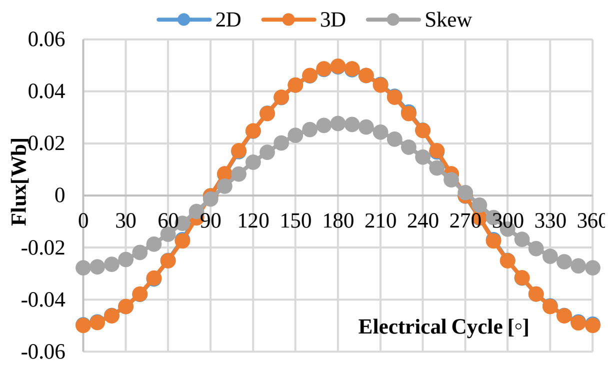

Figure 5: U-phase flux linkage of 2D, 3D and skew rotor at Je of 30A/mm^2

B. Flux Linkage

Figure 5 illustrates the U-phase flux linkage in the armature coil for 2D, 3D and skew rotor structure at different DC FEC field current densities, J_e is also investigated. The maximum magnitude of flux linkage of 2D, 3D and skewed rotor were obtained with the values of 0.049Wb, 0.049Wb and 0.027Wb, respectively at field current density, J_e of 30A/mm^2.

C. Back Electromotive Force (EMF)

The performance of back EMF waveform of 2D, 3D and skewed rotor at field current density, J_e of 30A/mm^2 is shown in Figure 6. The amplitude of 2D analysis was obtained at 273.40V, 3D is 272.54V and the skewed rotor is 148.56V, respectively. Back-EMF is produced as a result of the relative motion between the magnetic field and the coil. However, the back-EMF waveforms are not purely sinusoidal due to harmonics content especially for 2D and 3D analysis.

D. Harmonic of Back EMF

Figure 7 illustrates the harmonic amplitude percentage of back-EMF with the harmonic order at field current density, J_e of 30A/mm^2 for 2D, 3D and skewed rotor. The highest value was obtained at 7th harmonic order with the percentage of 3.43% for 2D analysis, while for 3D analysis the highest percentage is obtained at the 11th harmonic order with the value of 4.09%. Furthermore, the skewed rotor yields the highest magnitude of harmonic at the 13th harmonic order which is 2.16%. The lowest value of the harmonic order was obtained at 3rd, 9th and 15th harmonic for 2D, 3D and skewing rotor, respectively. The harmonic content has distorted the back-EMF waveform and as a result, the waveform becomes not solidly sinusoidal.

E. Flux Distribution

Flux distribution analysis is also carried out at the maximum field current density, J_e of 30A/mm^2 for 2D, 3D and skewed rotor and the results obtained is shown in Figure 8(a), (b) and (c), respectively. It is clear that 50% of flux flowing into the rotor and another 50% of flux flowing in the stator. The flow of direction flux distribution is saturated at high density and cancellation at a low of magnetic flux density.

F. Torque Characteristics at Various Current Densities

The graph in Figures 9(a), (b) and (c) show the torque characteristic versus field current density, J_e at various armature current, J_a of 2D, 3D and Skewing. The J_e will increase the torque to a certain load of J_a. The 2D and 3D graph states that the Ja of 5A$_{rms}$/mm^2 and 10A$_{rms}$/mm^2 is applied, the torque raise from J_e of 5A/mm^2 until Je of 20A/mm^2 and started to drop the torque with a small range when the J_e increase from 25A/mm^2 to Je of 30A/mm^2 is utilized. Then, J_a of 15A$_{rms}$/mm^2 and 20Arms/mm2 is applied, the torque raises from J_e of 5A/mm^2 until Je of 25A/mm^2 and started to drop the torque with a small range

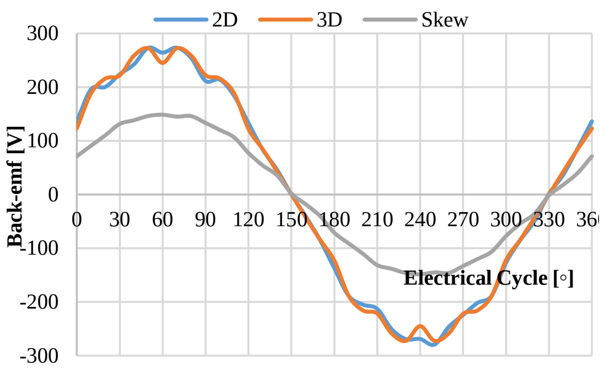

Figure 6: Back-EMF of 2D, 3D and skew rotor at J_e of 30A/mm^2

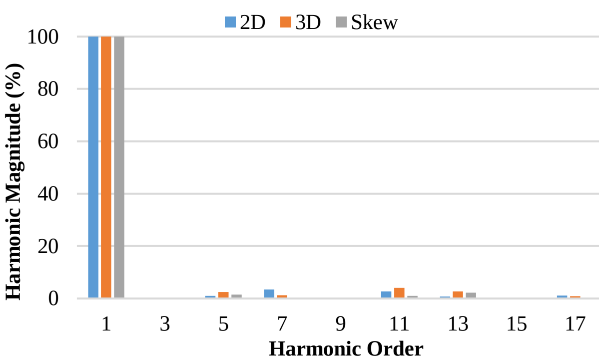

Figure 7: Harmonics content of 2D, 3D and skew rotor at J_e of 30A/mm^2

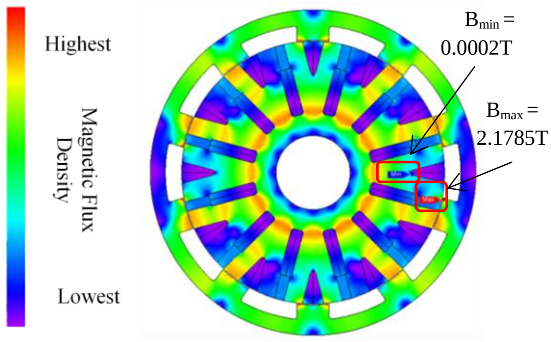

Figure 8 (a): Flux distribution of 3D at J_e of 30A/mm^2

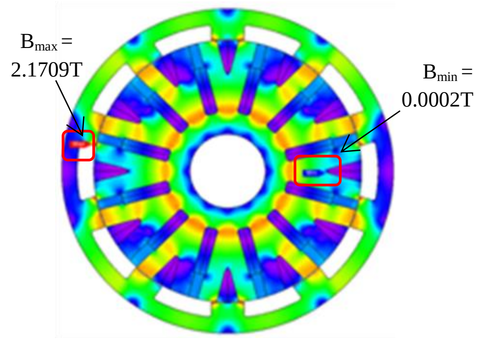

Figure 8 (b): Flux distribution of 3D at J_e of 30A/mm^2

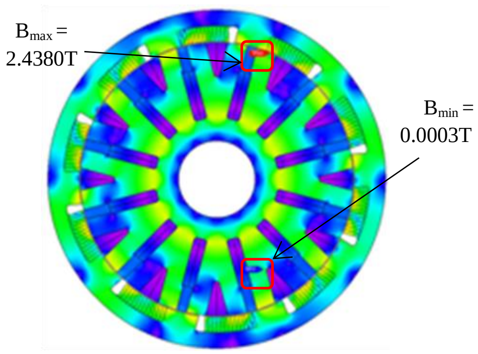

Figure 8 (c): Flux of distribution skewing at J_e of 30A/mm^2

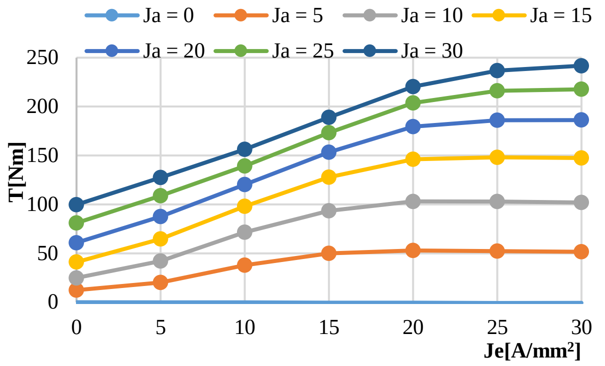

(a)

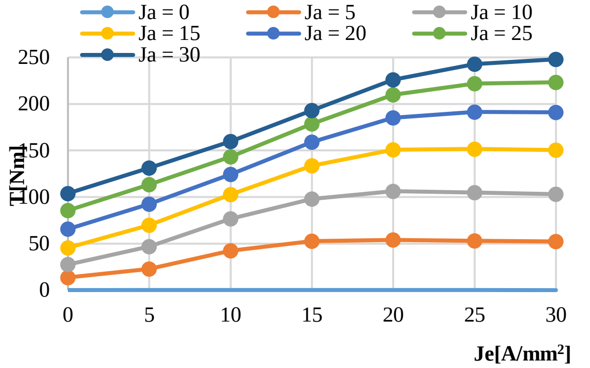

(b)

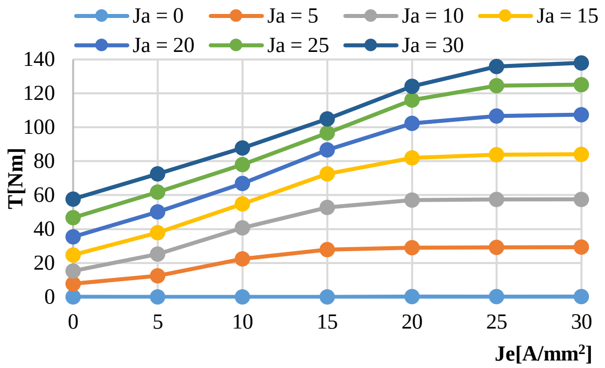

(c)

Figure 9: Torque versus J_e at various at various current J_a density condition of (a) 2D, (b) 3D and (c) skewing rotor

of J_e increases to the 30A/mm^2. Finally, the J_a of 25A$_{rms}$/mm^2 and 30A$_{rms}$/mm^2 is applied, the torque raises from J_e of 5A/mm^2 until J_e of 30A/mm^2. The skewing graph states that the J_a of 5A$_{rms}$/mm^2 until 30A$_{rms}$/mm^2 is applied, the torque increases from J_e of 5A/mm^2 to J_e of 30A/mm^2. From the graph, we can say that when Ja is set at a maximum of 30A$_{rms}$/mm^2, and J_e is to 30A/mm^2, the torque kept increased from the highest value is 241.77Nm in 2D, 247.95Nm in 3D and 138.03Nm in skewing.

G. Torque and Power versus Speed

The graph in Figure 10 shows the torques versus speed of 2D, 3D and skew rotor of OR-HEFSM. The 2D values for a speed increase of 0 rpm to 5719.49 rpm and the torque were the highest with a constant value of 242.75Nm. Then, the speed keeps increasing until 14,580.19rpm whereas the torque starts to decrease until 104.57Nm.

The 3D values for a speed increase of 0 rpm to 5752 rpm and the torque were the highest with a constant value of 248.33Nm. Then, the speed keeps increasing until 21,529 rpm whereas the torque starts to decrease until 105.56Nm. The skewing rotor value of speed increase from 0 rpm to 5958 rpm and the torque was the highest with a constant value of 138.03Nm. Then, the speed keeps increasing until 16,793 rpm whereas the torque starts to decrease until 61.70Nm. It shows that the higher the value of torque, the smaller the value of speed. So, it means this motor is suitable for the electric vehicle.

Figure 11 shows that the power versus speed graphs of 2D, 3D and Skewing. The 2D value of speed increasing from 0 rpm to 14,580 rpm whereas the maximum power obtained is 159.66kW. The 3D value of speed increasing from 0 rpm to 14,726.57rpm whereas the maximum power obtained is 162.79kW. The skewing rotor value of speed increasing from 0 rpm to 16,793 rpm whereas the maximum power obtained is 108.513kW.

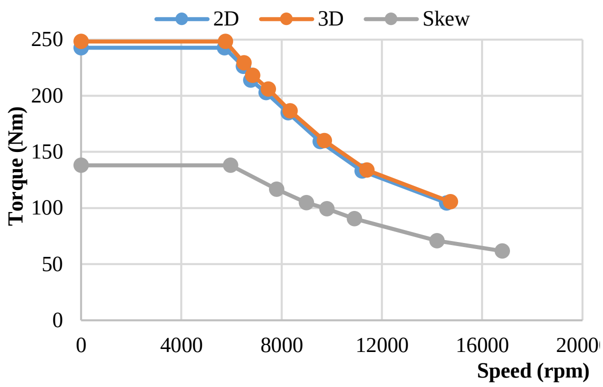

Figure 10: Torque versus speed of 2D, 3D and skew rotor

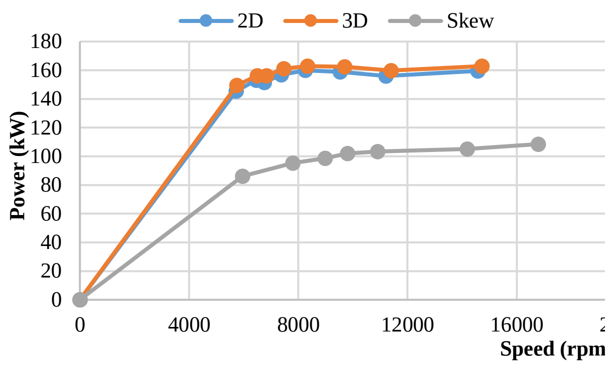

Figure 11: Power versus speed of 2D, 3D and skew rotor

IV. CONCLUSION

In this paper, the performance of OR-HEFSM at no load and the loaded condition has been analyzed and implemented using JMAG-Designer of finite element software. The results obtained show that the skewing method implemented on the rotor has greatly improved cogging torque by 91% reduction compared to the original design. In addition, the reduction of cogging torque, it has significantly enhanced the quality of the back-emf signal in which the harmonic content only occurs at 5th, 11th, and 13th harmonic order with small value compared to the original OR-HEFSM.

ACKNOWLEDGMENT

This work was supported by IGSP (Vot. U683) under Ministry of Education Malaysia, and Universiti Tun Hussein Onn Malaysia (UTHM), Batu Pahat, Johor, Malaysia.

REFERENCES

[1] M. Z. Ahmad, E. Sulaiman, G. M. Romalan, M. Jenal and T. Kosaka, "Three-phase variable flux outer-rotor switched flux permanent magnet machine," in *2016 XXII Int. Conf. on Electrical Machines (ICEM)*, pp. 2563-2569, 2016.

[2] M. Z. Ahmad, E. Sulaiman, Z. A. Haron and T. Kosaka, "Design improvement of a new outer-rotor hybrid excitation flux switching motor for in-wheel drive EV," in *2013 IEEE 7th Int. Power Engineering and Optimization Conf. (PEOCO)*, pp. 298-303, 2013.

[3] M. M. A. Mazlan, E. Sulaiman, M. Z. Ahmad and S. M. N. S. Othman, "Design optimization of single-phase outer-rotor hybrid excitation flux switching motor for electric vehicles," in *2014 IEEE Student Conf. on Research and Development*, pp. 1-6, 2014.

[4] M. Jenal, E. Sulaiman, M. Z. Ahmad, F. Khan and M. F. Omar, "A new alternate circumferential and radial flux (AlCiRaF) permanent magnet flux switching machine for lightweight EV," *2016 XXII Int. Conf. Electrical Machines (ICEM)*, pp. 2399-2405, 2016.

[5] G. M. Romalan, E. Sulaiman, M. Z. Ahmad, M. F. Omar and M. K. Hassan, "Structural and assembly design of outer-rotor hybrid excitation flux switching motor based on finite element analysis approach," in *2015 IEEE Conf. on Energy Conversion (CENCON)*, pp. 305-309, 2015.

[6] M. Z. Ahmad, Z. A. Haron, E. Sulaiman and T. Kosaka, "Design studies on 125-10p outer-rotor HEFSM for in-wheel drive EV applications," in *2013 IEEE Conf. on Sustainable Utilization and Development in Engineering and Technology (CSUDET)*, pp. 46-51, 2013.

[7] F. Khan, E. Sulaiman, M. F. Omar and M. Jenal, "Performance comparison of wound field flux switching machines," in *2015 IEEE Conference on Energy Conversion (CENCON)*, pp. 310-314, 2015.

[8] E. Sulaiman, T. Kosaka, N. Matsui and M. Z. Ahmad, "Design studies on high torque and high power density hybrid excitation flux switching synchronous motor for HEV applications," in *2012 IEEE Int. Power Engineering and Optimization Conf.*, pp. 333-338, 2012.

[9] M. M. A. Mazlan, E. Sulaiman and T. Kosaka, "Design study of single phase outer-rotor hybrid excitation flux switching motor for hybrid electric vehicles," in *2014 IEEE 8th Int. Power Engineering and Optimization Conf. (PEOCO2014)*, pp. 138-143, 2014.

[10] E. Sulaiman, N. S. M. Amin, Z. A. Husin, M. Z. Ahmad and T. Kosaka, "Design study and analysis of hybrid excitation flux switching motor with DC excitation in radial direction," in *2013 IEEE 7th Int. Power Engineering and Optimization Conf. (PEOCO)*, pp. 40-45, 2013.